Proceedings of International Conference on Heat Exchanger Fouling and Cleaning - 2011 (Peer-reviewed)
June 05 - 10, 2011, Crete Island, Greece
Editors: M.R. Malayeri, H. Müller-Steinhagen and A.P. Watkinson

Published online
www.heatexchanger-fouling.com

EVOLUTION OF BIOFOULING ON HEAT TRANSFER SURFACE CAUSED BY SIMULATED TREATED SEWAGE: INFLUENCE OF CALCIUM IONS

L. Tian[1], Q.P. Yang[1], L. Shi[1], J.C. Chen[2]

[1] Key Laboratory for Thermal Science and Power Engineering of Ministry of Education, Tsinghua University, Beijing 100084,China; tian-l07@mails.tsinghua.edu.cn
[2] School of Life Sciences, Tsinghua University, Beijing 100084,China

ABSTRACT

Heat pump using treated sewage water as heat source and sink was employed at Beijing Olympic Village to supply heating and cooling, which is an effective way to reuse urban waste heat. However, fouling occurs in plate heat exchangers of the heat pump. In the current study, an experimental system, which mimics the treated sewage water and simulates the relevant fouling formation process, has been developed to investigate the influence of Ca^{2+} on biofouling properties. Extensive experimentation including process monitoring and microstructure development in biofilm have been conducted and presented in this paper with the view of attempting to reduce fouling in future. A series of quantitative information has been obtained and discussed. The results show that the interactions between the microorganisms and Ca^{2+} clearly influenced the biofilm development thus impacting on the thermal resistance created. It was found that influence of Ca^{2+} on biofouing differs at different formation stages.

INTRODUCTION

Sewage is an important carrier of urban waste energy, which contains large low-grade heat. Treated sewage can be used as a suitable heat source in the heat pump system, which is an effective way to save energy and protect the environment during heating and cooling (Funamizu et al., 2001). Treated sewage source heat pump system has been introduced into Beijing Olympic Village District Heating & Cooling in 2008 (Shi and Zan, 2008).

Treated sewage contains some components causing fouling, such as heterotrophic bacteria, microbial nutrients and suspended substance. These could not be completely removed during treatments conducted by wastewater treatment plant. Thus fouling inevitably occurs in heat exchangers of the treated sewage source heat pump system. Fouling on the heat exchanger surface is a composite material consisting of biological and inorganic fouling (Shi et al., 2009; Zan et al., 2010). It is further demonstrated that biofouling is the major part of the fouling, which affect the fouling properties dramatically (Ma et al., 2010). The dynamic behavior of biofouling on the heat transfer surface is essential to character the development of composite fouling caused by treated sewage. The quantitive correlations of the heat transfer resistance and friction resistance produced by biofouling, biofouling mass and morphology is needed to improve the anti-fouling strategies.

Ca^{2+} concentration in treated sewage varies at different locations, and even varies over time in some wastewater treatment plants due to the injection of industrial sewage. It is known that Ca^{2+} has significant effects on the biological fouling (Characklis, 1990; Geesey et al., 2000; Lattner et al., 2003). Ca^{2+} can promote both specific and non-specific interactions with protein and polysaccharide adhesion molecules at the cell surface, and influence the attachment processes by acting as important cellular cations and enzyme cofactors; Ca^{2+} has the effect on electro-static interactions between cell and substrum surface, and impacts the mechanical properties of biofoulings (Fletcher, 1988; Geesey et al., 2000; Sheng et al., 2008). However, few studies are available on the effect of Ca^{2+} on biofouling that is related to heat transfer efficiency (i.e. the increase of fouling heat transfer resistance and friction resistance) under the conditions close to actual heat exchangers in a real heat pump energy recovery system using treated sewage water.

The purpose of the study was to investigate the influence of Ca^{2+} on biofouling properties. The paper presents the results obtained with biofoulings formed by a treated sewage water analog, which was made of a mixture aqueous suspension of Bacillus subtilis bacteria and Ca^{2+} flowing under turbulent conditions. The correlations between the heat transfer resistance, friction resistance, mass and morphology of biofouling were discussed.

MATERIALS and Methods

A comprehensive assessment system was developed to simulate the treated sewage heat exchange system. The schematic diagram is given in Fig.1. The apparatus handles the model fluids, which had the defined components, to flow though a plate heat exchanger (PHE) and two flow cells (rectangular stainless steel channel). These all served as fouling sections. Under different Ca^{2+} concentrations, the development of the heat transfer resistance caused by biofouling formed in the PHE was continuously recorded. Meanwhile, the flow cell was designed to allow extraction of stainless steel coupons giving direct measurements of the biofouling accumulated on the surfaces, which can be used

to figure out the fouled mass, surface roughness and make observations of the morphology of the fouled materials.

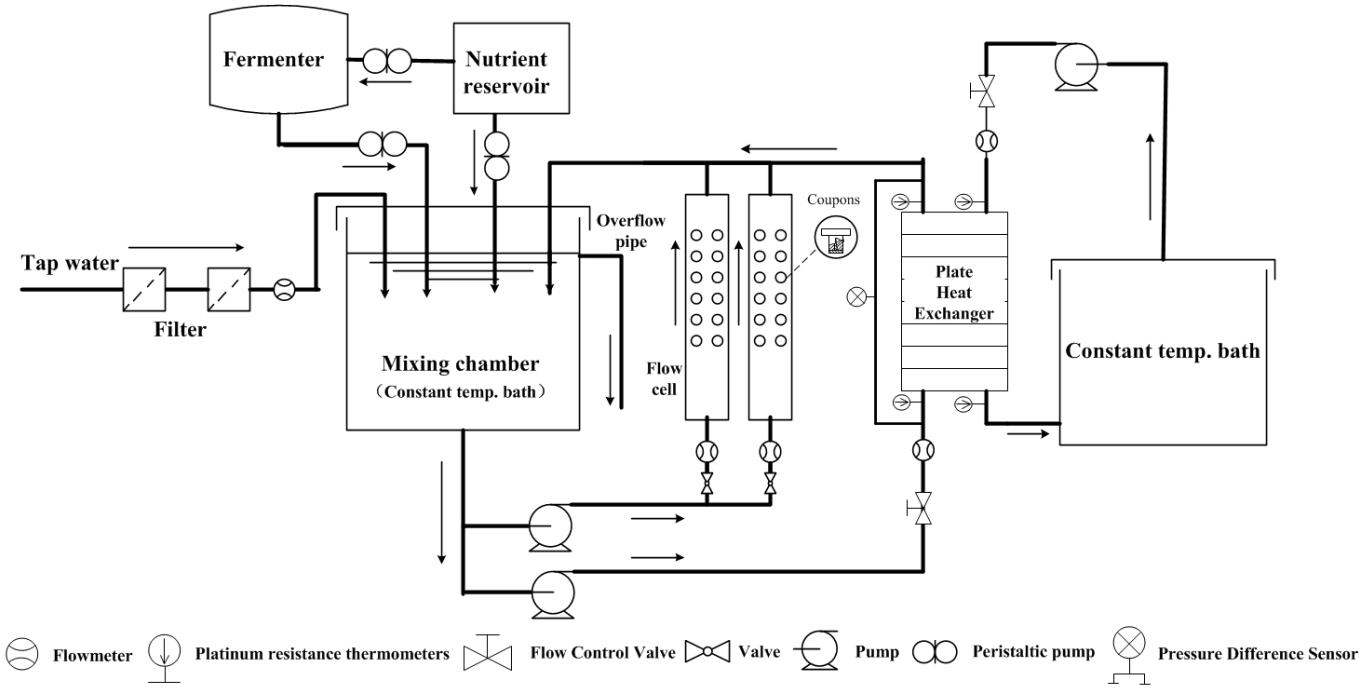

Fig.1 Diagram of the comprehensive assessment system

Model fluid

Treated sewage is composed of large volumes of water, a certain amount of organic pollutants and inorganic substances and some quantities of microorganisms. According to a one year-round monitoring of four large-scale wastewater treatment plants in Beijing, the concentration of total bacteria in treated sewage changed from 2×10^4 colony forming units (CFU) ml^{-1} to 7×10^4 CFU ml^{-1}. The concentration of the Ca^{2+} concentration ranged between 70 and 500mg L^{-1}.

Because the fact that the actual sewage is still too complicated to allow a good scientific study on various fouling factors, even though it is treated. A wastewater analog was made up to simulate the treated sewage with more defined components (Bott and Miller, 1983; Teodósio et al., 2011). To simulate closely the treated sewage, the model fluid was made up with four streams of water, Ca^{2+} solution, microorganism suspension and nutrient solution, with each stream having a defined composition.

The model bacterium used in this study, Bacillus subtilis, was isolated from the fouling formed on a plate heat exchanger running in the treated sewage source heat pump system which provided heating and cooling for Beijing Olympic Village District. The bacterium was cultured in the nutrient broth medium with 0.5% glucose (Belitsky, 1998) using a chemostat (BioFlo 110, New Brunswick Scientific Inc., USA). The pure culture of Bacillus subtilis was drawn off the chemostat by a peristaltic pump to inoculate the water sample in the chamber, and to give a final concentration of 5×10^4 CFU ml^{-1}.

The sterile broth medium was fed using a peristaltic pump. The medium was composed of glucose (0.5%), peptone (1%), beef extract (0.5%) and NaCI (0.5%) in distilled water. The medium was sterilized at 121 °C.

$CaCI_2$ (Sinopharm, China) dissolved in deionized water was used to adjust Ca^{2+} concentration in the mixing chamber. Ca^{2+} concentration was determined colorimetrically by a photometer with calcium hardness reagent (Photometer 7500, Palintest, UK).

Two filters (5μm / 0.15μm) were employed in the system to sterilize large quantities of water. Then the water was continously filled into a 15 L reservoir which acted as the mixing chamber for the four mentioned earlier. The flow rate of water into the apparatus was set at 15 L h^{-1}, giving a residence time in the system of 1h. A recirculation system is used in which the model fluid was recirculated through the PHE and the flow cells. In order to minimize concentration gradients along the system, the total residence time in the present system was 66.6 s.

The fouling section

Pleat heat exchanger

The plate heat exchanger employed in the current experimentation had 11 pieces of chevron-type plate, made of AISI 316 stainless steel with the thickness of 0.5 mm. The corrugation spacing between plates was 5mm, corresponding to a hydraulic diameter of 8.75 mm approximately. In the experiment, the model fluid at 26℃ was pumped into the plate heat exchanger to give a velocity

of about 0.4 m s^{-1} between plates. The temperature increase on the model fluid side from the inlet to the outlet was 5℃. On the other side, clean water was fed at 35℃ and at the same rate, recording a temperature drop from the inlet to the outlet of 5℃.

Flow cell

Two flow cells that are capable of inserting coupons were constructed to simulate the flow in the plate exchanger. Each flow cell was assembled by two removable stainless steel plates (ANSI 316), and the inside channel dimension was 800mm×35 mm×5 mm (a rectangular channel), corresponding to a hydraulic diameter of 8.75 mm, the same as the PHE. The treated sewage thus flowed upwards through the vertical flow cell. On one side of the channel there were twenty step-holes used to inject coupons, and the other one side had ten step-holes. The flow field of the flow cell was simulated using the software package Fluent (version 6.0, ANSYS Inc., USA). It was validated that the distance from the entrance to the first coupon met the length requirements for full development of the flow (Bakker et al., 2003) by analysis of velocity profiles and by monitoring the wall shear stresses distribution. The nonuniformity of the flow field where coupons were located in could be ignored in the velocity range of 0.1-2.5 m·s^{-1}.

The coupons (ANSI 316) were 6±0.1 mm in diameter and 60±20 mg in weight. *Ra* roughness of the end surfaces was 0.4±0.1 μm (tested using a surface mapping microscope, Micor XAM, ADE, USA) in accordance with the plates in the plate heat exchanger.

The flow cells and the PHE were subjected to the same thermal and hydraulic conditions as the plate heat exchanger, and the cells allowed individual sampling of each coupon without disturbing the biofilm formed on the others. Numerous testing experiences gained on this aspect to suppose this statement (unpublished observations).

Measurement methods

Mass of fouling

Biofouling formed at the coupons embedded in the flow cells were weighed and observed. Firstly, all the coupons were cleaned, dried, weighed and observed, to give the initial weight and surface morphology prior to fouling; at regular intervals (one day) during the biofouling development, three coupons evenly distributed in the flow cell were removed and placed in a temperature humidity chamber (DHG-9035A, Zhonghuan, China) for 30 minutes at 30□ to remove the excess water, subsequently the coupons were weighed, so that the difference in the two measurements was the dry fouled mass. The fouled mass per unit surface area (M_f, g m^{-2}) can be determined by Eq. 1.

$$M_f = \frac{m_f - m_c}{s} \quad (1)$$

The weight of fouled material was measured using an analytical balance (0.0001 mg accuracy, XP2U, METTLER TOLEDO Inc., Switzerland). After weighing, the distribution of the composite fouled material at the top surface of the coupon was recorded by a research stereomicroscope system (SZX16, Olympus, Japan).

Heat transfer resistance of biofouling

Heat transfer resistance [R_f (m^2 K W^{-1})] was used to obtain the characterization of fouling formed in the plate heat exchanger (Characklis et al. 1990). Heat transfer resistance indicates the sum of the resistance to heat transmission, and its values depend on the accumulation of biofouling. It was defined by

$$U = \frac{Q\rho c_p \Delta T}{A\Delta T_m} \quad (1)$$

$$R_f = \frac{1}{U_f} - \frac{1}{U_c} \quad (2)$$

Where U(W m^{-2} K^{-1}) is the overall heat transfer coefficient, Q (m^3 s^{-1})is the fluid flow rate, ρ(kg m^{-3}) is the fluid density, c_p is the specific heat at constant pressure, ΔT (K) is the temperature difference between the inlet and outlet of test fluid, A is the heat transfer surface area (m^2), ΔT_m (K) is the logarithmic mean temperature difference between the test fluid and the clean water. The subscript *c* represents the initial clean status and *f* represents the biofouling formation status.

The temperature and flow rate of the model fluid and the clean water were continuously measured by platinum resistance thermometers (±0.15℃, PST, Keyi, China) and flowmeters (±0.3%, AXF, Yokogawa, Japan). Ball valves were used for flow distribution; the accurate control of flow rate was carried out by the flow control valves (Hydromat Q, Oventrop Inc., Germany).

Frictional resistance of biofouling

The friction resistance caused by biofouling accumulated in the plate heat exchanger was monitored by a differential gage (±0.1% accuracy, EJX, Yokogawa, Japan) installed between inlet and outlet. The differential pressure (ΔP) is directly proportional to the surface friction factor under the same hydraulic conditions (i.e. flow velocity is kept constant) in the fixed heat exchanger (Albert et al., 2011), and the ratio of the pressure drop with respect to the initial value [Ψ (%)] was used to present the frictional resistance caused by biofouling.

$$\Psi = \frac{\Delta P_f}{\Delta P_c} \times 100\% \quad (5)$$

Where ΔP_c (Pa) is the initial value of pressure drop, and ΔP_f (Pa) is the pressure drop after biofouling formed.

Observation methods on biofouing morphology development and roughness

The evolution of the surface morphology of biofouling was observed by Environment Scan Electron Microscope (ESEM) (Quanta 200 FEG, FEI Inc., USA) under wet mode. Since ESEM does not require specimens to be metal-coated or stained, non-invasive imaging can be performed on surfaces in their native states and under near-physiological conditions. To observe the biofouling surface morphology, the coupons were replaced on a daily basis during biofouling development, and all coupons were removed simultaneously to observe at the end of the entire experiment. The *Ra* roughness was measured by the surface mapping microscope (Micor XAM, ADE, USA), and five determinations for each coupon were done to obtain the averages.

Investigation on the effects of Ca^{2+}

To investigate the effect of Ca^{2+} on biofouling, the plate heat exchanger and the flow cells exposed to the model fluids with Ca^{2+}concentrations of 70, 200 or 500 mg L^{-1},respectively. 70mg mg L^{-1} is the natural background Ca^{2+} concentration of local groundwater. 200 mg L^{-1} is the Ca^{2+} concentration of treated sewage reused, and 500 mg L^{-1} is the peak value. The velocity in the plate heat exchanger and the flow cells was set as 0.4 m s^{-1}, which was similar to that in the plate heat exchangers running in Beijing Olympic Village heat pump system. The experimental conditions are listed in Table 1. The curves lasted for 14 days to establish the preliminary stage of biofouling development. After each run of test, the flow system was first washed by NaClO solution, and rinsed by the filtered water for three times.

Table 1. Experimental conditions

Condition	Experimental object	Equivalent diameter (mm)	velocity m·s^{-1}	Bacterium CFU/ml	Temperature ℃	Ca^{2+} concentration (mg/L)
#1	PHEs	≈8.75	0.4	5×10^4	26℃	70
	channel	8.75				
#2	PHEs	≈8.75				200
	channel	8.75				
#3	PHEs	≈8.75				500
	channel	8.75				

Statistical analyses

The data presented were averages of the triplicate sets for each of the conditions, repeated measures analysis of variance was used to examine the influence of Ca^{2+} concentration on biofouling growth. Paired t-test analysis was used, each time point was evaluated individually using the triplicate sets obtained. It was considered significant at the level $P\leqslant0.05$, the time points were marked with an ●.

RESULTS

Developmental of biofouling resistances

Fig. 2(a) illustrates the biofouling heat transfer resistances with time in the plate heat exchanger under three concentrations of Ca^{2+}. During the first three days, the heat transfer resistances under three conditions had few differences. The influence of Ca^{2+} was weak. And then Ca^{2+} exposed its role, different Ca^{2+}concentrations brought about different biofouling resistance changing rates. The higher the Ca^{2+} concentration was, the faster the changing rate increased, so the disparities appeared. On day 13, the biofouling resistances under Ca^{2+} concentration of 500mg/L, 200mg/L, 70mg/L reached to 2.3, 1.9 and 0.5 m^2 K W^{-1}, respectively. The disparities with respect to the biofouling heat transfer resistance under 70mg/L were 4.6 and 3.8 times.

Fig. 2(b) illustrates the ratios of the pressure drop with respect to the initial value with time in the plate heat exchanger under three concentrations of Ca^{2+}. The variation trend of the pressure drop was similar with that of heat transfer resistance. On day 13, the increases of pressure drops under Ca^{2+} concentration 500 mg L^{-1}, 200 mg L^{-1}, 70 mg L^{-1} reached to 190%, 145% and 111% with respect to the clean heat exchanger (the pressure drop on day 0), , respectively. The disparities with respect to the pressure drop ratio under 70mg/L were 1.7 and 1.3 times.

It should also be noted that the grow rates of the heat transfer resistance and the pressure drop changed during the whole experimental period, hence it could be concluded that there were different stages in the time-varying process of biofouling resistances, and the influence of Ca^{2+} on stages is the key to explain the results.

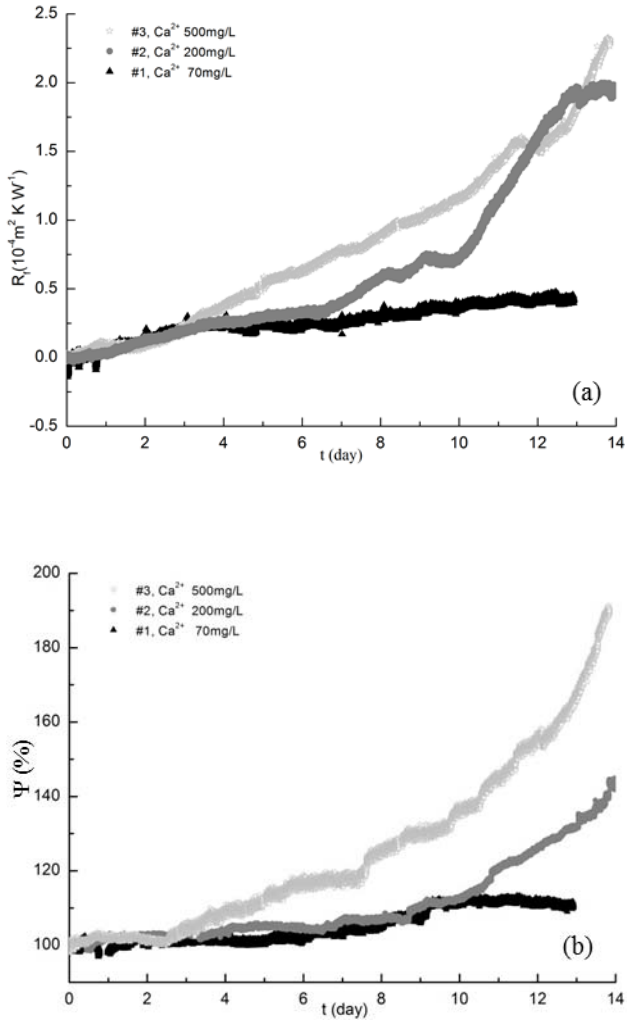

Fig.2 Development of the heat transfer resistances (a) and the ratios of the pressure drop with respect to the initial value (b) in the plate heat exchanger under different Ca^{2+} concentrations. The relative error of R_f was below 6% according to the date error analysis.

Growth curves of biofouling

Fig. 3 illustrates the increased biofouling masses with time under different Ca^{2+}concentrations. During the first three days the biofouling masses and growth rates under three Ca^{2+} concentrations had few differences, and then the biofouling grow rates increased and showed different values, hence the biofouling mass disparities appeared, which were consistent with the biofouling resistances. On day 13, the biofouling masses under Ca^{2+} concentration of 500mg L^{-1}, 200mg L^{-1}, and 70mg L^{-1} reached to 21.3, 13.0 and 5.2 g m^{-2}, respectively. The disparities with respect to the biofouling mass under 70mg/L were 4.1 and 2.5 times.

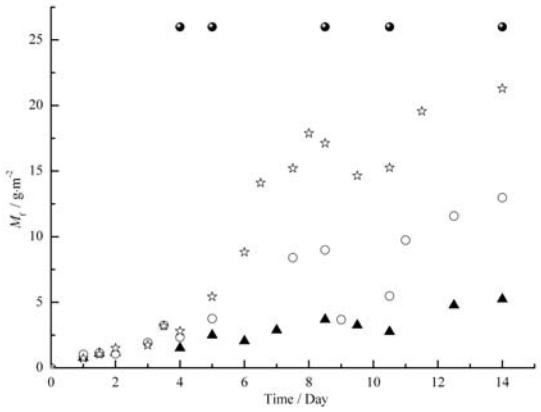

Fig.3 Growth curves of biofouling under different Ca^{2+} concentrations (triangular symbols - 70mg/L Ca^{2+}, open circle symbols -200mg/L Ca^{2+}, star symbols - 500mg/L Ca^{2+}). The results were averages of the triplicate sets for each of the conditions; an average standard deviation below 12% was obtained for the biofouling mass. Statistical analysis corresponding to each time point was represented with ● for a confidence level greater than 95% ($P \leqslant 0.05$).

Biofouling morphology

Biofouling morphology was observed via ESEM after 2, 7 and 12 days, and the images were shown in Fig.4. Bacterial colonization was heterogeneous in space and time under different Ca^{2+} concentrations. For biofouling formation in 70mg/L Ca^{2+}, single cells and small colonies consisting of a few cells were observed on days 2 and 7, a dense bacterial populations layer with protuberances occurred on day 12. In 200mg/L Ca^{2+}, the layer arose on day 7, filamentous structures were observed on day 12. In 500mg/L Ca^{2+}, after the filamentous structures on day 7, net-shape structures appeared on day 12. The evolution of biofouling morphology showed three differentiated phases, which could be characterized by single cells and small colonies, colonization layer with protuberances, and filamentous and net-shape. The demarcation points were different under three Ca^{2+} concentrations.

Surface roughness

The surface roughness changed over time as shown in Fig. 5. The surface roughness changed with the evolution of biofouling structure. The attached cells and the followed small colonies filled the unevenness of the coupon surfaces, which reduced the surface roughness; along with the process of colonization layer with protuberances formed, the surface roughness reached the minimum value and then increased; the formation of filamentous and net–shape increased the surface roughness, which contributed a higher roughness in the suitable conditions. During the development of biofouling, the heat transfer surface changed from stainless steel to biofouling, the change of the roughness affected the neat wall flow velocity and the followed the heat transfer resistance and flow resistance.

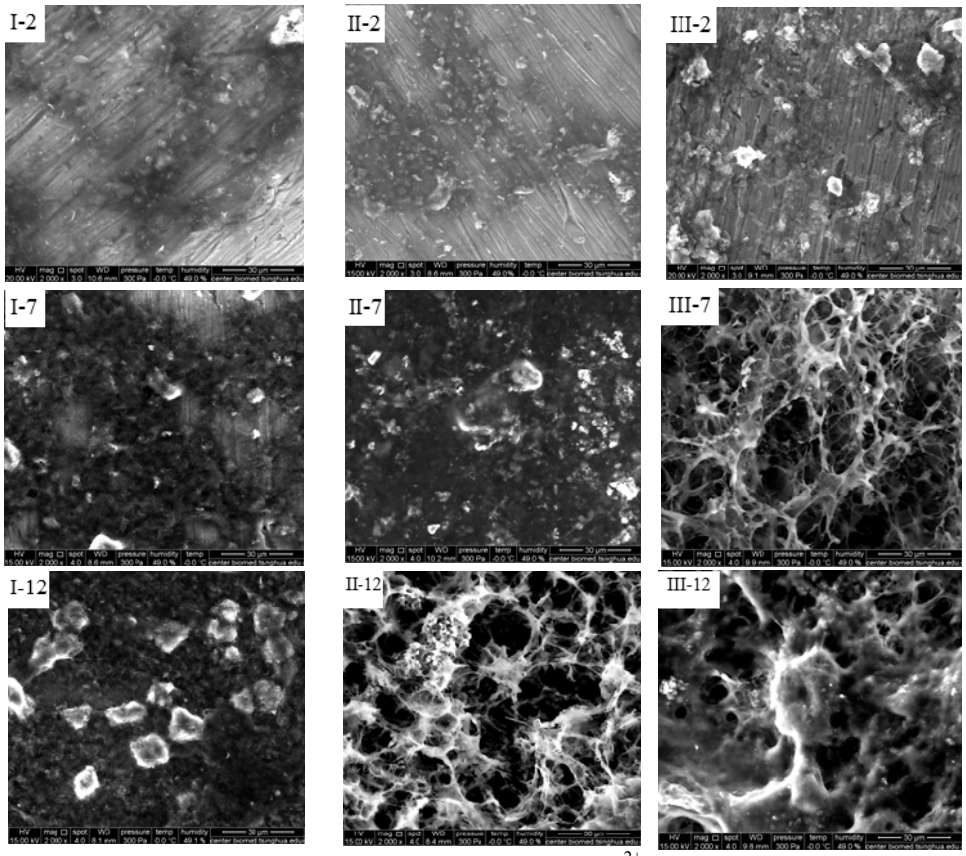

Fig.4. Biofouling morphology under ESEM grown in different Ca^{2+} concentrations on days 2, 7 and 12.

DISCUSSION

The development of biofouling on the heat transfer surface affects three aspects: the accumulation of insulating layers formed by the biofouling, which are directly related to the biofouling mass; the change of surface roughness produced by biofouling morphology; the decrease of flow section due to the biofouling established. All of these affect thermal performance as well as fluid dynamic of the heat exchanger.

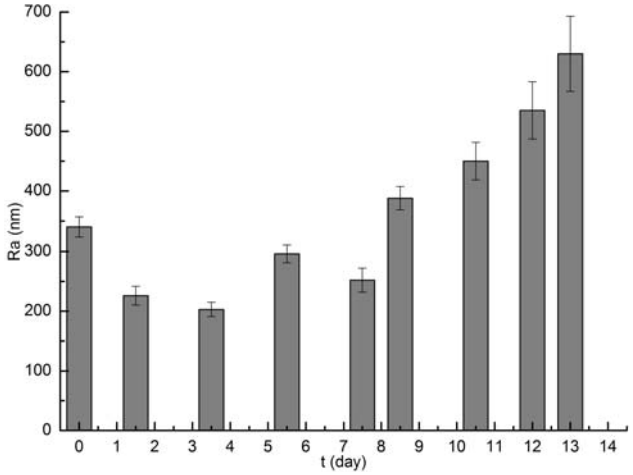

Fig. 5 Surface roughness of the flow cell with time under Ca^{2+} concentration of 200mg/L. Values are means + standard errors (n=5).

The formation process of biofilm consists of several steps (O'Toole et al., 2002; McLandsborough et al., 2006): (i) transport, (ii) initial adhesion, (iii) substrate attachment, and (iv) microcolony formation (cell–cell adhesion), leading to the mature biofilms consisting of cells and a surrounding extracellular polymeric substances matrix. The initial phase in biofilm formation consists of the transport and sorption of individual microbial cells to clean surface, and Ca^{2+} is considered to play an important role in adhesion of cells to surface (Fletcher, 1988; Geesey et al., 2000; Lattner et al., 2003). However, the result showed that biofouling masses within 24h under three Ca^{2+} concentrations had few differences; one reason may be that the influence of Ca^{2+} dependent on substratum chemistry and flow conditions, at the same time and not all bacteria display enhanced adhesion with increasing cation concentration (Hoogmoed et al., 1997). During this period, the biofouling layer was thin that the biofouling cannot affect the flow section and the heat transfer resistance is small. The surface roughness affects the flow regime at the border layer, which changes heat transmission by convection.

After they had colonized the surface, microorganisms began to form the microcolony and the followed flat monolayers of cells (Fig. 4) by synthesizing extracellular polymeric substances (EPS) that facilitated irreversible bacterial attachment to a surface and help maintain the structure (Sutherland et al, 2001), and the biofouling mass increased gradually. EPS have been shown to enhance

nutrient capture and resistance to environmental stress (Jenkinson and Lappin-Scott, 2001; Costerton et al., 1995) which boosts the metabolism of bacteria. Consequently the biofouling mass increased rapidly, and filamentous structures and the followed net-shape were formed (Fig. 4). These structures are an important part of the propagation mechanisms and have shown to have substantially different densities than the base biofilm (Loosdrecht et al., 1997).

The differences of biofouling masses under the three Ca^{2+} concentrations were noteworthy after the initial phase, which proved the important influence of Ca^{2+} on biofouling grow. The growth of the biofouling is mainly due to the activity of microorganisms located in the attached film (Bott and Miller, 1983), Ca^{2+} can facilitate the production of EPS (Costerton,1995), and EPS enhances the nutrient capture, so Ca^{2+} accelerates the growth rate and favors the bioflouing mass. At the same time, it was showing high concentration of Ca^{2+} was effective to accelerate the evolution of biofoling morphology (Fig. 4), the role of Ca^{2+}can be attributed to act as a significant cross linker of the biofouling matrix and contribute to properties of the lipopolysaccharides (Geesey et al., 2000; Koerstgens et al., 2001). Ca^{2+}can reduce the repulsive force between negative groups on the polysaccharides, which constitute the structure of biofouling (Costerton, 1995) in combination with the facilitation in EPS production.

Undoubtedly, the increase of biofouling mass is the base of heat transfer resistance and flow resistance. However, compared with the development of biofouling heat transfer resistance and flow resistance, it should be paid special attention to the differences between the biofouling mass growth rate and the fouling resistance growth rate, biofouling heat transfer resistance and flow resistance showed more dramatic changes than the biofouling mass, so heat transfer resistance and flow resistance were not only the function of biofouling mass, biofouling structure should be taken into consideration. As shown in Fig. 2 and Fig. 4, the rapid growth of biofouling heat transfer resistance during day 7 to day 12 under 200mg/L matched up to the formation of the net-shape structure; similarly, the change of biofouling resistance during day 2 to day 12 under 500mg/L was coincided with the formation and consolidation of the net-shape; further, under 70 mg/L it didn't form the net-shape until day12 so that the growth rates of the heat transfer resistance and friction resistance were low and the heat transfer resistance and friction resistance were small. It can be concluded that the biofouling morphology is an important factor which affects the biofouling heat transfer resistance and flow resistance.

CONCLUSIONS

A comprehensive assessment system which simulates the treated sewage heat exchange system has been developed to study the dynamic behavior of biofouling on the heat transfer surface. Development of biofouling heat transfer resistance and friction resistance were obtained under three Ca^{2+} concentrations, the corresponding growth curves of biofouling were obtained through weight differences. The evolution of biofouling morphology was observed via ESEM. The influence of Ca^{2+} on the process of biofouing formation varies over time. An initial stage with a low fouling growth rate exists at the beginning, and the influences of Ca^{2+} concentrations are weak. After the preliminary stage, the different concentrations of Ca^{2+} bring about different biofouling growth rates. The influence of Ca^{2+} on the heat transfer resistance and friction resistance is the synthesis result which affects both the biofouling mass and biofouling morphology.

NOMENCLATURE

A heat transfer surface area, m^2
c_p fluid specific heat at constant pressure, kJ kg^{-1} K^{-1}
U heat transfer coefficient, W m^{-2} K^{-1}
Q fluid flow rate, m^3 s^{-1}
Ra surface roughness, nm
R_f heat transfer resistance, m^2K W^{-1}
T fluid temperature, K
ΔT_m Logarithmic mean temperature difference, K
ΔP differential pressure, Pa
Ψ the ratio of the pressure drop at time t to the initial pressure drop (t=0), %
ρ fluid density (kg/m^3)

Subscript
c clean status
f fouling formation status
in inlet
out outlet

REFERENCES

Albert, F., Augustin, W., and Scholl, S., 2011, Roughness and constriction effects on heat transfer in crystallization fouling, *Chem. Eng. Sci.*, Vol.66, pp.499-509.

Bakker, D.P., Mats, van der A., Verkerke, G.J., Busscher, H.J., and Mei, van der H.C., 2003, Comparison of velocity profiles for different flow chamber designs used in studies of microbial adhesion to surfaces, *Appl. Environ. Microbiol.*, Vol.69, pp.6280-6287.

Belitsky, B.R., and Sonenshein, A. L., 1998, Role and regulation of Bacillus subtilis glutamate dehydrogenase genes, *J. Bacteriol.*, Vol.180, pp.6298-6305.

Bott, T.R., and Miller, P.C., 1983, Mechanisms of biofilm formation on aluminum tubes. *J. Chem. Technol. Biotechnol.*,Vol.33, pp.177-184.

Costerton, J.W., 1995, Overview of microbial biofilms. J. Ind. Microbiol. Vol.15, pp.137-140.

Costerton, J.W., Lewandowske, Z., Caldwell, D.E., Korbre, D.R., and Lappin-Scott, H.M., 1995, Microbial biofoulings, *Ann. Rev. Microbiol.*, Vol.49, pp.711-745.

Characklis, W.G., and Mrshall, K.C., 1990, *Biolilms*, Wiley, New York, USA.

Fletcher, M., 1988, Attachment of Pseudomonas fluorescensto glass and influence of electrolytes on bacterium-substratum separation distance, *J. Bacteriol.*, Vol.170, pp, 2027-2030.

Funamizu, N., Lida, M., Sakakura, Y., and Takakuwa, T., 2001, Reuse of heat energy in wastewater: implementation examples in Japan, *Water Sci. Technol.*, Vol.43, pp.277-285.

Geesey, G.G., Wigglesworth-cooksey, B., and Cooksey, K.E., 2000, Influence of calcium and other cations on surface adhesion of bacteria and diatoms: a review, *Biofouling*, Vol.15, pp.195-205.

Hoogmoed, van C.G., Mei, van der H.C., and Busscher, H.J., 1997, The influence of calcium on the initial adhesion of S. thermophilus to stainless steel under flow studied by metallurgical microscopy, *Biofouling*, Vol.11, pp.167-176.

Jenkinson, H.F., and Lappin-Scott, H.M., 2001, Biofilms adhere to stay, *Trends Microbiol.*, Vol.9, pp.9-10.

Koerstgens, V, Flemming, H.C., Wingender, J., and Borchard, W., 2001, Influence of calcium ions on the mechanical properties of a model biofouling of mucoid Pseudomonas aeruginosa, *Water Sci. Technol.*, Vol.43, pp.49-57.

Lattner, D., Flemming, H.C., and Mayer, C., 2003, 13C-NMR study on the interaction of bacterial alginate with bivalent cations, *Int. J. Biol. Macromol.*, Vol.33, pp.81-88.

Loosdrecht, van M.C.M., Picioreanu, C., and Heijnen, J.J., 1997, A more unifying hypthesis for biofilm structures, *FEMS Microbiol. Ecol.*, Vol.24, pp.181-183.

Ma, X.J., Zan, C., An, Q.S., Guo, J. and Shi, L., 2010, Experimental study of the initial period of fouling growth in municipal secondary effluent system, *J. Tsinghua Univ. (Sci. Technol.)*, Vol. 50, pp.274-277.

McLandsborough, L., Rodriguez, A., Pérez-Conesa D., and Weiss, J., 2006, Biofilms: At the Interface between Biophysics and Microbiology, *JFOBI*, Vol.1, pp.94-114.

O'Toole, G., Kaplan, H.B., and Kolter, R., 2000, Biofilm formation as microbial development, *Annu. Rev. Microbiol.*, Vol.54, pp.49-79.

Sheng, X., Ting, Y., and Pehkonen, S.O., 2008, The influence of inoic strength , nutrients and pH on bacterial adhesion to metals. *J. Colloid Interface Surface*, Vol.321, pp.256-264.

Shi, L., and Zan, C., 2008, Large-scale application of municipal reclaimed water source heat pump to a DHC system in the Beijing Olympic Village, *9th IEA Heat Pump Conference*, Zurich.

Shi, L., Zan, C., and Yang, W.Y., 2009, Composition and morphology of composite fouling by municipal secondary effluent on heat transfer surfaces, *J. Tsinghua Univ. (Sci. Technol.)*, Vol.49, pp.240-243.

Sutherland, I.W., 2001, The biofilm matrix—an immobilized but dynamic microbial environment. *Trends Microbiol.*, Vol.9, pp.222-227.

Teodósioa, J.S., Simõesa, M., Melo, L.F., and Mergulhão, F.J., 2011, Flow cell hydrodynamics and their effects on E. coli biofilm formation under different nutrients and turbulent flow, *Biofouling*, Vol.27, pp.1-11.

Zan, C., Shi, L., Yang, W.Y., and Ma, X.J., 2010, Evolution of composite fouling on a vertical stainless steel surface caused by treated sewage, *Front. Energy*, Vol.4, pp.171-180.